To appear in:

Majlesi Journal of Electrical Engineering (MJEE)

Online ISSN: 2345-377X **Print ISSN:** 2345-3796

Received: 19/03/25

Revised: 10/06/25

Accepted: 25/06/25

DOI: 10.57647/j.mjee.2025.17717

Original Research

Modelling and Analysis of a Hybrid Photovoltaic-Thermoelectric Generator System using a Relative Humidity Adaptive Maximum Power Point Tracking Algorithm

Pallavi Roy[1], Bipul Kumar Talukdar[2], Sandip Bordoloi[3], Bani Kanta Talukdar[4]

1- Dept. of Electrical Engineering, Girijananda Chowdhury University, Guwahati, India

Email: pallavi_ee@gcuniversity.ac.in (Corresponding author)

2-Dept. of Electrical Engineering, Jorhat Engineering College, Jorhat, India

Email: bipulktalukdar@gmail.com

3- Dept. of Electrical Engineering, Girijananda Chowdhury University, Guwahati, India

Email: sandip_ee@gcuniversity.ac.in

4-Dept. of Electrical Engineering, Assam Engineering College, Guwahati, India

Email: bktalukdar@yahoo.com

Abstract

As the need for green energy intensifies, hybrid energy systems have emerged as promising solutions to improve power generation efficiency and reliability. Among these, Photovoltaic Thermoelectric Generator (PV-TEG) hybrid systems have attracted significant attention due to their ability to harness both solar irradiance and waste heat. Despite the progress in PV-TEG hybrid technologies, environmental factors such as relative humidity (RH) are often overlooked in system modelling and performance analysis. The present research develops a novel maximum power point tracking (MPPT) algorithm for a hybrid PV-TEG system integrating a humidity derating factor (HDF) and examines it in SIMULINK under diverse scenarios of solar irradiance, ambient temperature, and RH. Linear Regression is used to analyse corelations among the performance parameters of the hybrid system. Simulation results show that at 90% RH, the efficiency of the standalone PV system drops by 7%, while the same is improved by 12% in the PV-TEG hybrid model. The proposed humidity-adaptive MPPT algorithm based

on Perturb & Observe framework achieves convergence within 0.03 seconds per iteration with a total simulation runtime of 12.4 seconds for a full 24-hour environmental profile. The findings highlight the ability of the proposed PV-TEG system to sustain stable voltage and power output during environmental fluctuations; and underscore the importance of incorporating HDF in MPPT control.

Keywords: Humidity, Maximum power point tracking controller, Photovoltaic, Perturb and observe optimization, Thermoelectric generator

1. Introduction

The escalating global demand for energy, alongside rising environmental concerns and dwindling fossil resources, has created a pressing need for the development of clean, sustainable, and efficient energy solutions. Solar energy, due to its abundance and renewability, stands out as one of the most promising alternatives. Photovoltaic (PV) systems, which directly convert solar radiation into electrical energy, have seen significant growth in popularity over recent decades [1],[2]. However, their efficiency is constrained by various environmental and operational factors, with temperature being a paramount concern. [3],[4]. As the operating temperature of PV modules increases, their efficiency typically declines, attributable to the intrinsic characteristics of semiconductor materials [5],[6]. To mitigate the thermal inefficiencies associated with standalone PV systems, hybrid systems that integrate PV modules with thermoelectric generators (TEGs) have been proposed [7]. The PV-TEG systems capitalize on the waste heat released by PV panels. TEGs, which operate based on the Seebeck effect, can convert temperature differences directly into electrical power, thereby providing a complementary means of energy generation [8],[9]. The PV-TEG system not only enhances the overall energy conversion efficiency but also helps in managing the thermal profile of PV panels, potentially extending their operational lifespan [10],[11]. Existing literature has explored PV-TEG systems through both theoretical and practical approaches. Kamouny K. et al. demonstrated that incorporating a thermoelectric module into a PV panel significantly enhances the system's efficiency [12]. The sun's radiation that strikes the surface of PV panel and the temperature of the panel's surface are the two main determinants of PV output. The efficacy of a PV system improves in proportion to the increased solar radiation. However, the solar energy reaching the panel is impacted due to external factors such as dust build-up on the panel, shadowing across the panel's surface, and the presence of airborne contaminants or water vapour [13],[14]. As panel temperatures rise, key output metrics such as fill factor (FF), open-circuit voltage (V_{OC}), and maximum power (P_{max}) experience significant declines [15]. Furthermore, there is a slight increase in current I_{SC} with rising temperatures. Consequently, the PV panels' overall efficiency diminishes as their temperature increases. According to earlier

research, as the panel's temperature rises, its V_{OC}, drops at a rate of 0.45% per °C. Likewise, as the panel temperature increases, the output power and FF drop at steady rates of -0.65% and -0.2% per °C, respectively. Therefore, a detailed understanding of temperature in PV panel under different situations is important for the PV system to operate efficiently. For that, Lamda R. et al. proposes a concentrated PV-TEG hybrid system and caries out performance analysis for it [16]. A comprehensive review of such systems is also presented by Sahin A.Z. et al. [17] and Indira S.S. et al [18]. Qasim M.A. et al. explains how the heat produced during normal photovoltaic operation can be converted into useful energy with a hybrid PV-TEG set up [19]. Kohan H.F. et al. simulates a similar system to justify its effectiveness [20]. For further improvement in efficacy of PV-TEG system, integration of proper MPPT techniques is important [21]-[23]. This is addressed by Yang B. et al. carrying out a detailed review of MPPT for hybrid PV-TEG systems [24]. In another research, Brahmi M. et al. highlights comparative optimization strategies for MPPT controllers with partial shading conditions (PSC) [25]. Considering PSC, Bayat M. et al. outlines a hybrid intelligent global MPPT enabled algorithm [26]. Senapati M.K. et al. investigates intelligence-based algorithms for MPPT to optimize PV performance with PSC and temperature effects [27]-[30]. Ahmadi M. et al. explores harmonics detection with oscillatory coupling effect [31]. Again, fuzzy logic-based MPPT methodologies has been proposed for PV-TEG systems by Kanagaraj N. et al. in [32] and by Safaei K. et al. in [33]. Similar MPPT algorithms using PSO and P&O are suggested by Muhammed R. A. et al. [34] and Jaklair L. et al. [35] respectively.

Wu et al. explores the main challenges that continue to hinder the efficiency of TEG systems, despite recent technological advancements [36]. A significant issue identified is low conversion efficiency, primarily arising from difficulties in manufacturing processes, electrode connections, and material performance [36]. Dhawan et al. presents a model to improve the efficiency of microelectronic TEGs, which are often limited by parasitic electrical and thermal resistances, especially when using materials like silicon [37]. They emphasize that while power and efficiency cannot be maximized at the same time, optimizing the packing fraction is essential. The model integrates these parasitic effects and suggests an optimal packing fraction of 1-10%, significantly lower than current designs, to enhance μTEG performance in future applications [37]. Rad et al. evaluates the performance of small-scale and concentrated PV-TEG units using affordable, commercially available components [38]. It finds that incorporating phase change materials (PCMs) with paraffin-wax and copper-fins in concentrated PV-TEGs systems significantly boosts efficiency, achieving about 15.5% electrical efficiency, 37.4% thermal efficiency, and 16.7% energy efficiency, while reducing cell temperatures by over 20%. However, TEGs with nanofluids are economically unviable, as they lead to a 15-35% increase in energy costs [38]. Wang et al. focus on optimizing the configuration of a PV-TEG array using CDIWO algorithm to improve energy conversion efficiency and adaptability to varying environmental conditions [39]. They effectively address challenges like PSC and temperature changes while maximizing power output and system reliability [39]. To enhance understanding of moisture

behavior, Mitterhofer et al. presents a two-stage 2D Fickian diffusion model with better boundary conditions, critiquing traditional single 2D simulations [40]. Overall, it emphasizes the need to accurately model moisture ingress in PV systems, considering local microclimates and back sheet interactions [40].

Several similar studies have investigated the performance of hybrid PV-TEG systems accounting solar irradiance and ambient temperature, but in most cases, the role of relative humidity (RH) remains underexplored. RH significantly affects solar energy systems by influencing solar radiation transmittance, convective heat transfer, and the cooling characteristics of PV modules [41]. High RH can reduce solar irradiance on PV panels due to water vapour scattering and absorption, but it enhances convective cooling, alleviating some heat accumulation issues [42]. Additionally, the performance of TEGs, which require a sufficient temperature gradient between their hot and cold sides, can be indirectly impacted by RH through its influence on ambient temperature and heat dissipation rates.

The present study addresses the aforementioned research gaps by developing a novel MPPT algorithm for a hybrid PV-TEG system that accounts for RH along with the irradiance and temperature effects. The inclusion of the humidity derating factor (HDF) enhances the power extraction efficacy of the hybrid system. The Perturb and Observe (P&O) optimization strategies have been employed in the proposed MPPT algorithm, which is simulated in a MATLAB/SIMULINK environment for quantitative assessment of the proposed PV-TEG system under different humidity profiles.

2. Methodology

In this study, a PV-TEG hybrid model is developed and the P&O algorithm is applied for MPPT considering humidity derating factor (HDF). The system is observed for the effect of humidity, temperature, and solar radiation. Mathematical modellings of the subsystems are illustrated as follows:

2.1. Modelling of PV System

PV cells are the fundamental units of solar energy system that convert solar radiation into electrical energy. Accurate performance prediction of such devices requires the modeling of nonlinear PV cell behavior, especially when it varies due to temperature and irradiance changes [2]. The double-diode model gives a detailed representation of electrical feature of a PV cell, accounting for recombination losses and resistive effects [43]. The current (I) of a PV cell is defined by equation (1).

$$I=I_{PV}-I_{d1}\left[\exp\left(\frac{V+IR_s}{\alpha_1 V_{T1}}\right)-1\right]-I_{d2}\left[\exp\left(\frac{V+IR_s}{\alpha_2 V_{T2}}\right)-1\right]-\left(\frac{V+IR_s}{R_P}\right) \quad (1)$$

where,

I_{PV}: Current related to a PV source in Ampere

I_{d1}: Scaling coefficient related to the first temperature-dependent component in Ampere

I_{d2}: Scaling coefficient related to the second temperature-dependent component in Ampere

V: Voltage across the system in Volt

R_s: Resistance in Ohms

α_1: Temperature coefficient for the first component(unitless)

α_2: Temperature coefficient for the second component(unitless)

T1: Temperature associated with the first component (unitless)

T2: Temperature associated with the second component in degree Celsius

R_P: Additional resistance or parameter related to the system in Ohms

The following equation characterizes the output current I_d of a PV cell, alongside the temperature dependence and the electrical characteristics of the cell [43].

$$I_d = \frac{(I_{SC\text{-}STC}+K_I\Delta T)}{\left[\exp\left(\frac{V_{OC\text{-}STC}+K_V\Delta T}{\alpha_1+\alpha_2}.\frac{\rho}{\Delta V_T}\right)-1\right]} \quad (2)$$

Where,

I_{sc-STC}: Short-circuit (SC) current of the PV cell under Standard Test Conditions (STC) in Ampere

K_I: Temperature coefficient for the SC current in Ampere/°C.

ΔT: Temperature gradient in °C.

$V_{OC\text{-}STC}$: Open-circuit (OC) voltage of the PV cell under STC in Volts

K_V: Temperature coefficient for the OC voltage in Volt/°C

$\alpha_1$and α_2: Temperature coefficients for specific components within the PV system. (unitless)

ρ: Resistivity (a material-specific parameter) of the PV components in Ωm

ΔV_T: Thermoelectric voltage per unit of temperature in Volt/°C

The PV cell's performance is depicted by the combination of $V_{OC\text{-}STC}$ and I_{SC-STC} in the equation (2) that models the output current of a PV cell. They are not, however, exactly proportionate. Rather, according to the diode equation, V_{oc} increases logarithmically with I_{sc}. Although both rise with increasing irradiance, they react differently to temperature: V_{oc} decreases noticeably with temperature, owing to increased carrier recombination, whereas I_{sc} tends to slightly increase. K_I, K_V, α_1, and α_2 indicate how PV cell parameters respond to temperature changes. These coefficients vary across different PV technologies due to material characteristics and cell structure. For example, thin-film technologies like CdTe or CIGS may exhibit lower K_V and sometimes a slightly positive K_I, while monocrystalline silicon modules typically have a higher V_{OC} and a moderately negative K_V (around –0.4 to –0.5%/°C). As a result, thin-film modules can retain a larger portion of their rated power in hotter conditions compared to crystalline modules [44]. These variations also affect simulation and prediction models.

The V_{OC} of a PV cell as a function of temperature change (ΔTn) between the junction (T_h) and the cell (T_c) is defined by equation (3). It demonstrates how temperature affects the output of a PV cell [2].

$$V_{oc} = K_V(T_h - T_c)n = K_V \Delta Tn \quad (3)$$

Equation (4) models the coefficient of temperature τ of the OC voltage of a PV cell at temperature T. [44]

$$\tau = T\frac{dK_V}{dT} \quad (4)$$

The terms 'K_V' and 'τ' both discuss how temperature impacts the functionality of thermoelectric and PV systems. The temperature coefficient of OC voltage, K_V is usually expressed in Volt/°C, while τ denotes the temperature-dependent variation of K_V and is measured in Volts.

Humidity can heavily impact efficiency by lowering it through scattering solar radiation and causing condensation, which reduces the amount of sunlight reaching the cell. The relation (5) is a basic approximation of a PV cell's efficiency under relative humidity (RH).

$$RH = \frac{100e}{e_s} \quad (5)$$

where, e is the actual water vapor pressure in the air and e_s refers the same-temperature saturation vapor pressure. The derating factor D_h is dependent on the RH. As humidity increases there is an increase in RH which leads to a higher humidity derating factor, $D_h(H)$ [42]. The efficiency considering relative humidity is given as in equation (6).

$$\eta_{PV}(H) = \eta_{PV,0} \times [1 - D_h(H)] \quad (6)$$

Where:

$\eta_{PV}(H)$: PV efficiency at a given humidity

$\eta_{PV,0}$: Baseline PV efficiency under standard conditions

2.2. Modelling of a TEG

Equation (7) gives the output power P_{TEG} of a TEG based on its electrical properties and resistance values.

$$P_{TEG} = \frac{(\alpha_{pn}\Delta T)^2 R_L}{(R_L + R_{TEG})^2} \quad (7)$$

Here, α_{pn} is the Seebeck coefficient. R_{TEG} is the internal resistance of the TEG in Ohms, which is inherently temperature-dependent owing to its temperature-sensitive resistivity (TSR). To ensure precise output, the TSR of TEG is integrated over the temperature gradient (ΔT) across the TEG. Load resistance, R_L is usually determined by the specific application and the desired operating point of the TEG. In practical scenarios, R_L is measured directly using standard electrical measurement techniques. Maximum power is attained when $R_L = R_{TEG}$, which is the well-known impedance matching condition. Deviations from this condition lead to decreased power output. To

optimize TEG performance, systems must maintain a large ΔT and utilize materials with low R_{TEG} and high α_{pn} [8]. Humidity alters heat transfer and produces condensation on TEG modules, which lowers ΔT. While moisture-induced corrosion damages material integrity and raises R_{TEG}, moist air's varying thermal characteristics affect cooling efficiency [9].

Humidity less impacts the TEG efficiency (η_{TEG}) than that by Seebeck effect. However, if humidity affects the cooling or heating elements of the TEG (such as through condensation or heat transfer efficiency), it can indirectly impact its overall performance. Thus,

$$\eta_{TEG} = \frac{\Delta T}{T_{avg}} \times ZT_{Material} \quad (8)$$

where, ΔT refers the temperature gradient across the TEG, T_{avg} is the average temperature, and $ZT_{Material}$ denotes the figure of merit of the TEG material and is dimensionless [45].

The total power-voltage efficiency (η_{PV-TEG}) of a hybrid PV-TEG system is given by,

$$\eta_{PV-TEG}(H) = \eta_{PV}(PV) + \eta_{TEG}[1 - Lh(H)] \quad (9)$$

where, $Lh(H)]$ is a loss factor that reflects the indirect effects of humidity on TEG performance [46].

2.3. Flowchart of the proposed MPPT

To enhance the power extraction efficacy of the hybrid system, the proposed MPPT methodology incorporates relative humidity as a critical factor alongside solar insolation and temperature. The P&O algorithm tracks changes in output power by gradually adjusting the actuating quantity, i.e., voltage or current. If power increases, the adjustment continues in that direction; if power decreases, it reverses direction. If the power output remains constant, the algorithm keeps the voltage unchanged. The procedure of the P&O based MPPT for the PV-TEG system incorporating humidity effect is demonstrated with a flowchart in Fig.1.

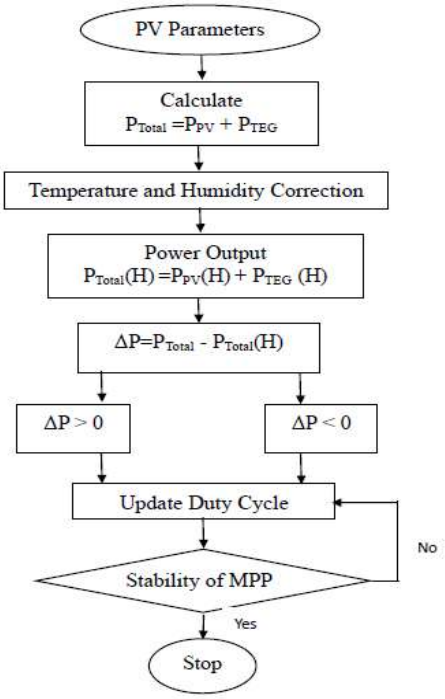

Fig.1: Flowchart of P&O based humidity adaptive MPPT for PV-TEG system

The P&O-MPPT algorithm is popular in real-world applications, particularly in small-scale or residential applications due to its low cost, simplicity, and reliable performance in stable conditions [41]. The present study employs this algorithm because of the aforesaid benefits; and highlights its effectiveness with a comparative analysis with other methods in Section 4.

3. Experimental Set-up and SIMULINK Model

The model in Fig. 2 illustrates a hybrid energy system combining PV and TEG technologies. The PV system captures solar energy, while the TEG converts thermal gradients into electricity. The model optimizes performance by analysing current, voltage, and power outputs. TEG outputs have been tested across 100 modules with varying temperatures and Seebeck coefficients. PV outputs are measured by adjusting solar irradiation and panel temperature with and without humidity effect.

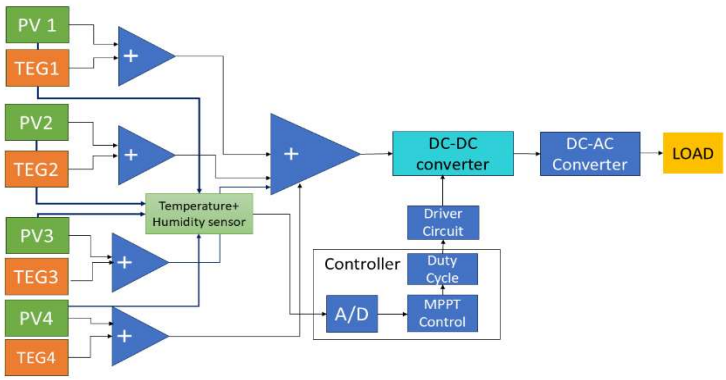

Fig.2: Hybrid PV-TEG model with humidity sensor and controller

The power from PV and TEG are added and transferred to the DC-DC converter. Temperature and humidity sensors continuously monitor the ambient conditions. These sensors provide signals to the MPPT controller, which adjusts the duty cycle of the converter. The output of the converter is sent to an inverter to supply AC power to the load.

Fig. 3 shows the SIMULINK model of the proposed PV-TEG system. It comprises of a PV array, a TEG subsystem, a DC-DC boost converter, a resistive load, and a P&O-MPPT controller. The P&O-MPPT framework dynamically modifies the duty cycle to track the optimum power point by using real-time V-I measurements from the

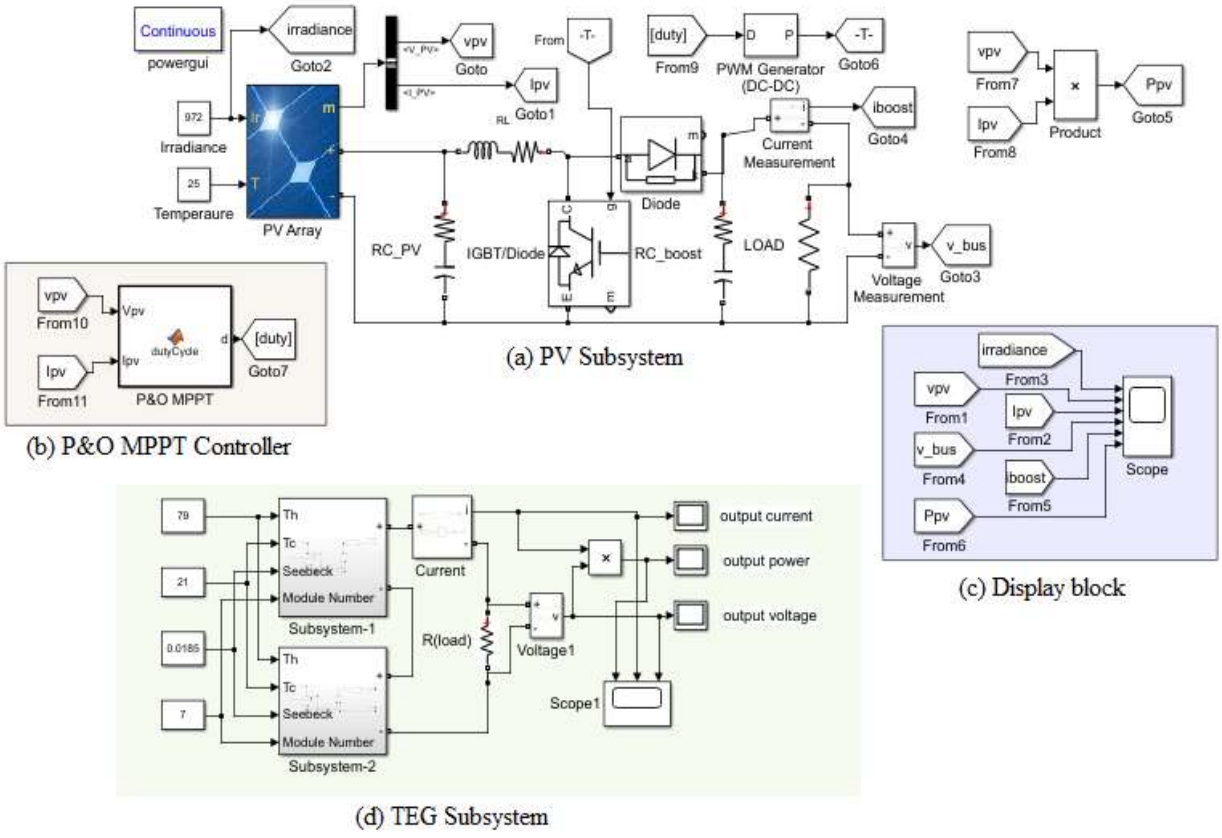

Fig 3: SIMULINK model of the P&O-MPPT controlled PV-TEG system under study

PV array. This duty cycle regulates the boost converter's IGBT switching, which improves the PV voltage while smoothing the output using an inductor and capacitor. After that, a resistive load receives the increased DC power. The system has measurement blocks for power, voltage, and current monitoring and scopes that display time-domain responses. For scalable and modular simulation, subsystems stand in for separate PV modules. Effective solar energy harvesting is made possible by this arrangement, which also exhibits dynamic adaptation through MPPT in a range of environmental conditions. Table 1 summarizes the specifications of the subsystems used in model.

Table 1. PV-TEG system components specification [47]

Subsystems	Specification
PV	Nominal Maximum Power (P_{max}):50Watts; V_{oc}: 21:9V; I_{sc}: 3:02A; Voltage at Max. Power (V_{mp}): 17:96V; Current at Max. Power (I_{mp}): 2:87A; Max. System Voltage: 1000V; Area of the PV panel: 0:3024m^2; FF: 0:77
TEG	Hot Side Temperatures: 25°C and 50°C; Q_{max}: 50 (at 25°C) and 57 (at 50°C); ΔT_{max}: 66°C (at 25°C) and 75°C (at 50°C); I_{max}: 6:4 Amps for both temperatures; V_{max}: 14:4 Volts (at 25°C) and 16:4 Volts (at 50°C); Module Resistance: 1:98 Ohms (at 25°C) and 2:30 Ohms (at 50°C); Seeback Coefficient: 53mV/K; Figure of Merit (ZT): 0:7
DC-to-DC Converter	Input: 12V; Output: 24-0-24V, Current: 10A
DC-to-AC Inverter	Battery capacity: 220mAh; Input Voltage (max): 25 V; Output power(max): 165W; Frequency: 50 Hz.

The control strategy presented in this work optimizes energy delivery from the PV-TEG hybrid system by employing a modified P&O MPPT algorithm integrated with HDF. This approach allows the controller to dynamically change with environmental variables, particularly RH. Instead of managing the PV and TEG units separately, the system focuses on their combined power output. The modified MPPT logic identifies the optimal voltage operating point for the entire array, allowing effective tracking of the MPP under varying conditions. This approach incorporates environmental feedback into the MPPT loop without adding complexity, ultimately enhancing energy yield.

4. Result and Discussion

The simulation results of the case studies performed in the PV-TEG system using the proposed humidity adaptive P&O- MPPT controller have been discussed in this section. The correlation of humidity with the PV-TEG system's performance parameters is analysed using linear regression. The outcomes of the analysis are categorized as follows:

(a) Effects of solar irradiance, temperature, and relative humidity on system performance
(b) Statistical analysis for the HDF integrated P&O-MPPT controlled PV-TEG system
(c) Performance analysis considering shading effect and humidity
(d) Comparative analysis of present study with existing literature

Fig. 4 shows how solar irradiation impacts the output voltage of all three systems. Increased radiation leads to higher photon absorption, which generates more electron-hole pairs and results in greater current flow. Additionally, this increase in radiation raises the temperature deviation in the hot and cold section of the TEG, thereby boosting the output voltage. Consequently, the combined PV-TEG system demonstrates improved performance, with the voltage rising from 16V to 39V as radiation levels increase.

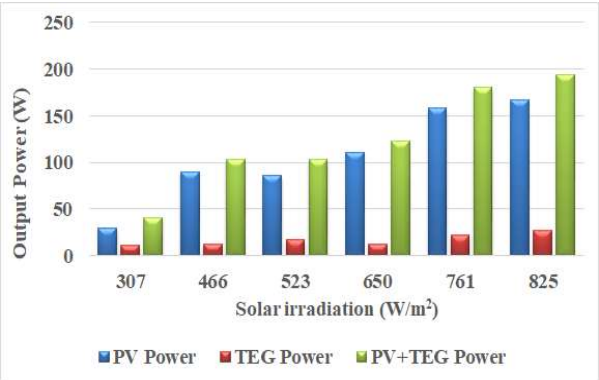

Fig.4 Effect of solar irradiance on output voltage

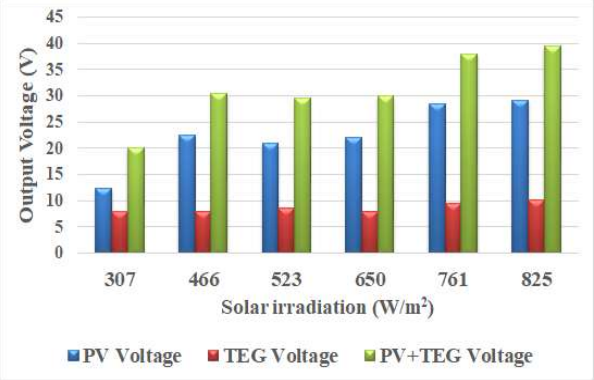

Fig.5 Effect of solar irradiance on output power

Similarly, Fig.5 justifies that the increase in solar radiation leads to enhanced output power for all three systems. The hybrid PV-TEG system delivers more power than the two individual systems at different irradiance levels. In Fig.6, it is evident that an increase in solar irradiation enhances the efficiency of PV systems by 6.9%. However, the elevated temperatures lead to thermal losses, which consequently decrease the efficiency of the TEG by 12%. This reduction has a further impact, resulting in an overall decrease in the efficiency of the hybrid system by 9%.

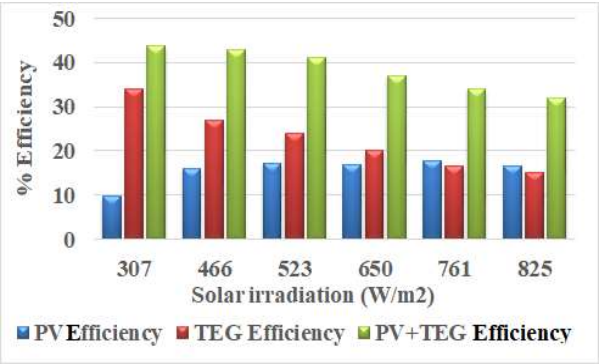

Fig. 6 Effect of solar irradiance on efficiency

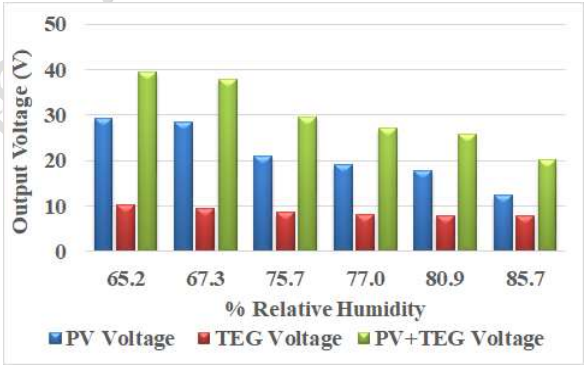

Fig. 7 Effect of relative humidity on output voltage

This data highlights the critical interplay between solar energy capture and thermal management in optimizing system performance. Although higher temperatures decrease efficiency, PV power output increases significantly from 40 W to 177W as solar irradiation increases, with voltage increasing to 3.75 mV per W/m². Rising temperatures in the hybrid PV-TEG system boost TEG output but also result in thermal losses, requiring the use of thermal management techniques like fins, heat sinks etc. to maintain system performance.

Fig. 7 demonstrates the effect of RH on the system's output voltage. It shows a drop in voltage from 29V to 12V for the PV system and from 5V to 3V for the TEG. The TEG voltage remains relatively stable, as RH has minimal impact on thermal conductivity within the hybrid system. Overall, the voltage reduced by 23V with an increase of 20.5% in RH, primarily due to the fall in PV performance.

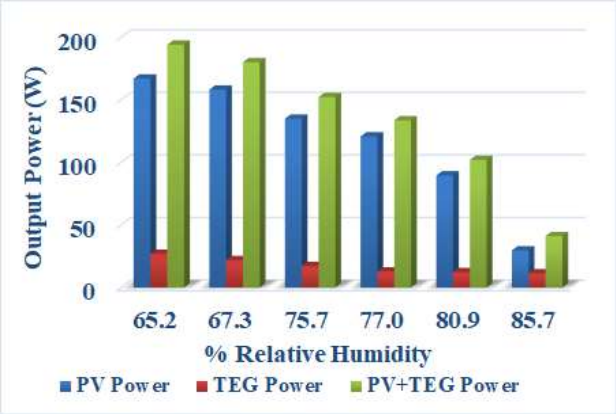

Fig.8 Effect of relative humidity on output power

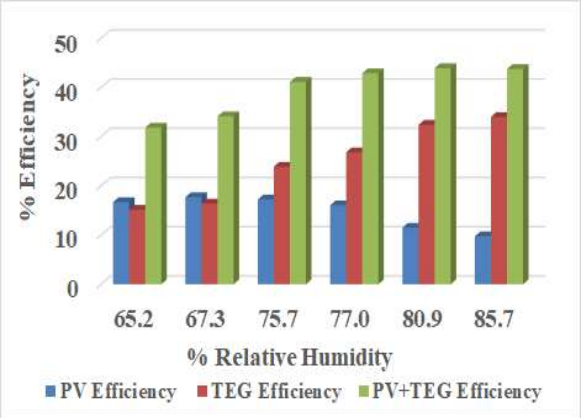

Fig.9 Effect of relative humidity on efficiency

Fig. 8 indicates that an increase in RH lowers the system's output power. This decrease is attributed to the increased atmospheric absorption and scattering of light caused by higher RH levels. While the total power of the PV-TEG hybrid system shows a declining trend, its output power remains greater than that of the two standalone systems. The efficiency of PV is reduced by 7%, while TEG efficiency increases by 17%. For the hybrid system, the efficiency enhancement is seen as 12%, as shown in Fig.9.

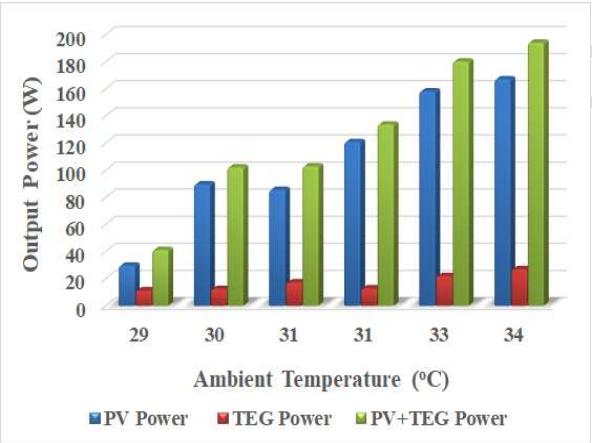

Fig.10 Effect of temperature on output voltage

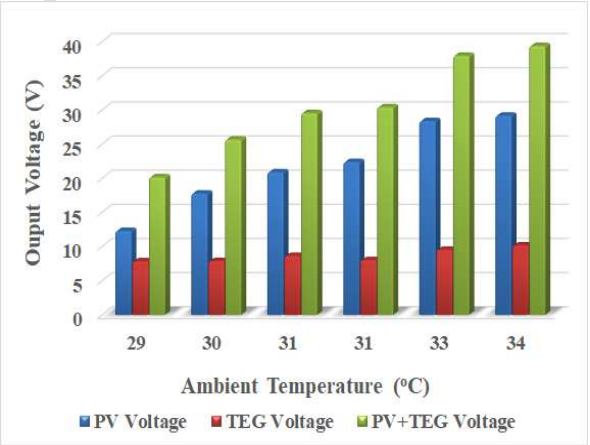

Fig.11 Effect of temperature on output power

Fig. 10 says that the voltage increase in the PV and TEG are 17V and 3V, respectively, with the rise in ambient temperature. In this hybrid system, the voltage increase is 23V. It has been found that when the temperature rises above 35°C, it negatively impacts cell temperature, thereby adversely affecting voltage output. However, when temperatures remain below 35°C, the voltage increases gradually as the cell temperature stays within the nominal operating range [4]. However, in Fig. 11, the output power increases as follows: for the PV system, it rises from 29W to 150W; for the TEG, it increases from 11W to 27W; and for the hybrid system, the power goes from 40W to 177W.

Fig. 12 shows the relationship between efficiency and ambient temperature. Efficiency initially increases with temperature but declines after reaching an optimal level for all three systems. This decline is due to higher temperatures raising cell temperature, which negatively affects efficiency. The PV-TEG hybrid system achieves higher efficiency than the standalone setups, peaking at 31°C.

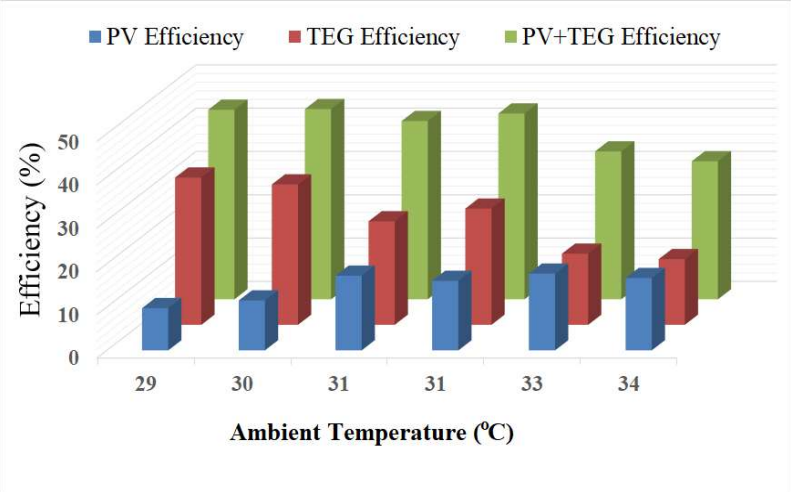

Fig. 12 Variation in system's efficiency with ambient temperature

Table 2 presents the statistical analysis of the system's performance parameters under diverse environmental constraints. It demonstrates that incorporating RH into the MPPT control strategy significantly influences the hybrid system's performance. By integrating a HDF into the power estimation and tracking process, the system more accurately reflects real operating conditions, leading to improved efficiency.

Table 2: A statistical analysis of results under diverse operating scenarios

Parameters	Solar Irradiation (W/m^2)	Relative Humidity (%)	Max. PV Output (W)	PV Efficiency (%)		Max. TEG Output (W)	TEG Efficiency (%)		PV-TEG Efficiency (%)	
				Without Humidity	With Humidity		Without Humidity	With Humidity	Without Humidity	With Humidity
Minimum value	95.0	60	51.6	9.8	1.9	45.9	8.7	1.7	18.5	3.7
Median value	148.0	70	51.6	10.5	3.5	45.9	9.2	2.4	19.9	6.7
Mean value	133.9	70	51.6	11.9	3.6	45.9	9.4	3.2	22.7	6.8
1st Quadrant	125.0	65	51.6	10.3	2.7	45.9	10.7	3.2	19.6	5.1
3rd Quadrant	150.8	75	51.6	12.5	4.1	45.9	11.1	3.7	23.6	7.8
Maximum value	159.0	80	51.6	16.4	6.6	45.9	14.6	5.8	31.0	12.4

Linear Regression [48] is used in this study to analyze the relationship between efficiency with and without the humidity factor in the proposed PV-TEG model. For the regression analysis, 1200 data have been prepared by taking the average solar insolation data from 2009 to 2024 (from January to December in kW/m^2) for the location (Latitude 26.133417 degrees and Longitude 91.621620 degrees). The global insolation data has been obtained using the ISRO Solar Calculator Application. The maximum and minimum temperatures of the PV and the TEG are taken from the average maximum and minimum temperature of the same region from January to December from 2009 to 2024 using the same application. The computational time for statistical analysis, including regression modelling over 1200 data points, is found to be less than 200ms. This indicates that the environmental correlation analysis and predictive performance evaluation are computationally light and appropriate for embedded applications

To use linear regression, the PV-TEG output power, solar insolation, and HDF have been taken as the independent variables, while the hybrid system efficiency with and without the HDF are taken as the dependent parameter. The findings show that while PV output decreases with higher humidity, the TEG can partially compensate by harvesting waste heat, resulting in a net gain in hybrid system's efficiency. This highlights the importance of environmental-aware control algorithms. Future PV-TEG systems can be optimized by adopting similar adaptive MPPT strategies that account for temperature, humidity, and irradiance, enabling more precise power tracking, better energy yield, and enhanced performance under diverse and dynamic environmental conditions.

The importance of the independent parameters on the dependent parameters has been tested using ANOVA (Analysis of Variance). Since the regression test has given two significant parameters only i.e. the solar insolation and HDF, the one way and two-way ANOVA tests have been employed. The one-way ANOVA test is used to determine the correlation of the Solar insolation with the Hybrid efficiency with humidity factor. It is observed that the hybrid efficiency has positive correlation as the p-value is $3.06x10^{-17}$from the Shapiro test for residuals and with the highest significant codes. Again, to test whether there is an interaction of hybrid efficiency with solar insolation and humidity, the two-way ANOVA test was performed. The test underlines that both solar insolation and humidity factor have a high correlation with the hybrid efficiency with the p-value $2.2x10^{-16}$ and F-value of 70002 and 118794 for solar insolation and HDF. The Shapiro-test for residuals gives p-value of $1.42x10^{-13}$. From the two-way ANOVA test, an interaction test was performed to test whether there is correlation between solar insolation and humidity factor. The interaction test has a p-value lower than $2.2x10^{-16}$, conclude that there is a strong correlation between these two independent factors, which in turn contributed to the strong correlation between the 'hybrid efficiency with humidity factor', and the 'solar insolation and HDF'.

The linear regression of the hybrid efficiency without HDF shows that there is no correlation of humidity, the maximum power of PV and TEG for the dependent variable i.e. hybrid efficiency with HDF. This means that these two parameters act independently. Although humidity does not

have a corelation with the hybrid efficiency and power, it does show a strong corelation when humidity is combined with solar insolation. The p-value is less than $2.2x10^{-16}$. The RMSE value is 0.00147 and the R-squared value is 0.98345. Since no correlation is shown by the humidity with the dependent parameter, only the one-way ANOVA test was carried out between the hybrid efficiency without humidity and the solar efficiency. The said test informs that there is a strong correlation of the solar insolation and the dependent parameter, having the p-value $\text{less than } 2.2x10^{-16}$. The Shapiro test for residuals gives the p-value to be $1.5x10^{-23}$.

Based on the regression model analysis of the 1200 data (prepared by taking the average solar insolation data from 2009 to 2024 in kW/m^2), partial irradiance's impact on the efficiency of the hybrid PV-TEG system is examined with and without humidity factor. The shading percentages in the test are 20%, 40%, 60%, and 80%, alongside a relative humidity (RH) level of 40% and 80%. Since there is no correlation between the maximum output power of the PV system and TEG with the efficiency of the hybrid PV-TEG system under humidity conditions, these two factors have been excluded from this analysis. The predicted efficiencies, elucidated in Table 3, provide a clear visualization of how partial shading and varying RH levels differentially influence the operational efficacy of the hybrid system. This articulation enables a better understanding of the intricate dynamics inherent in the hybrid PV-TEG design and lays a foundation for future research endeavours aimed at optimizing system performance across diverse environmental conditions.

Table 3. Efficiency of the hybrid PV-TEG system with shading effect

Shading Percentage	Solar Irradiation (W/m^2)	Efficiency without humidity (%)	Efficiency with 40% humidity (%)	Efficiency with 80% humidity (%)
20	104.8	23.20	21.20	18.60
	86.4	21.40	19.40	16.80
	80.0	19.80	17.80	15.30
40	78.6	18.10	16.10	13.60
	64.8	16.50	14.40	12.20
	60.0	14.90	13.00	10.70
60	52.4	13.20	11.50	9.30
	43.2	11.70	10.20	7.90
	40.0	10.50	8.60	6.80
80	26.2	8.30	6.90	5.20
	21.6	6.90	5.60	4.30
	20.0	6.20	5.00	3.80

Table 4 provides a comparative analysis of the proposed humidity-adaptive P&O-MPPT algorithm alongside several pertinent methodologies. It shows that the Roach Infestation

Optimization (RIO) [26] algorithm outperforms others in efficiency, convergence speed, and robustness. GEPSO [49] also demonstrated high efficiency (99.9%) and stable performance under dynamic conditions, though slightly slower than RIO.

Table 4: Comparison of present algorithm with the alternative methodologies

Algorithm	**Efficiency (MPPT)**	**Tracking Time / Convergence**	**Oscillations / Stability**	**Robustness (PSC, Load, Noise)**	**Source**
P&O with Humidity Derating Factor	97 – 98 % of true MPP (field-averaged) Hybrid efficiency more than 12%	Slow in rapid changing scenarios	Medium (some oscillation)	Medium (sensitive to humidity, not partial shading conditions (PSC)	Present Study
Metaheuristics (PSO,GA,AOA)	Up to 99.5% (varies by type)	Varies (Fast for PSO/GA/AOA)	Medium to low	High (Metaheuristics best under PSC/NTD)	[24]
Modified Adaptive Jaya Optimization (MAJO)	The MAJO algorithm enhances tracking efficiency by dynamically adjusting its parameters	Rapid convergence to the Global MPP, due to the adaptive nature of MAJO	Minimizes oscillations around the MPP, ensuring a stable and consistent power output.	Robust performance under PSC and varying load scenarios. Ensures consistent tracking performance in environmental disturbances.	[27]
Bio-Inspired	HHO and GWO achieve higher efficiency than P&O, effectively tracking the Global MPP under varying conditions	Faster convergence to the Global MPP, reducing the system settling time after environmental changes.	Both HHO and GWO minimize oscillations around the MPP, ensuring a stable and	Robustness to varying irradiance and temperature conditions,	[29]

			consistent power output		
RIO (Roach Infestation Optimization)	99.19% (uniform) 99.86% (PSC)	~58 ms (fastest in group)	Very low (most stable)	Very high (PSC, noise, load variation)	[30]
Fuzzy Logic	High and stable efficiency from startup to steady-state. Outperforms P&O and Incremental Resistance (INR) methods	Fast convergence to MPP	Very low oscillations around the MPP	Robust performance under load variation and temperature step changes	[32]
GEPSO	99.90%	0.29s – 0.57s	Very low (smooth, fast settling)	High (handles PSC, temperature shifts)	[49]
Mismatch Analysis	Not evaluated	Not applicable	Not applicable	Emphasizes need for robust MPPT	[50]
ANFIS	98.34%	Moderate to Fast	Stable	robust to environmental changes	[51]

The proposed humidity-adaptive MPPT algorithm based on P&O framework achieves convergence within 0.03 seconds per iteration with a total simulation runtime of 12.4 seconds for a full 24-hour environmental profile. It has moderate convergence speed; however, it is significant and novel because it dynamically modifies the operating point in response to real-time humidity variations, which are known to affect PV module performance due to their effect on temperature regulation and surface condensation, in contrast to conventional methods that assume fixed environmental conditions or limit adaptations to irradiance and temperature. In addition to increasing field-averaged efficiency to 97–98%, the present approach outperforms standard P&S in hybrid system applications by more than 12%. Traditional methods like P&O with a humidity factor improve adaptability but lag in speed and accuracy.

5. CONCLUSION

In this paper, a hybrid PV–TEG system that incorporates a humidity-adaptive traditional P&O based MPPT algorithm is presented. In order to compensate for environmental losses that conventional irradiance-temperature models lack the ability to compensate for, the proposed method adds a simple humidity derating factor (HDF) that dynamically modifies the duty cycle response based on relative humidity. In comparison to traditional P&O, the suggested method achieves up to 12% higher energy yield, with tracking efficiency approaching 98%, as shown by simulation results across a range of climatic scenarios (irradiance 200–1000 W/m^2, temperature 20–45 °C, and relative humidity 30–90%). Additionally, the algorithm converges to the MPP in 0.4 seconds under standard test disturbances, maintaining a minimal computational footprint suitable for implementation on affordable microcontrollers. The humidity-compensated P&O achieves a practical balance between accuracy, speed, and hardware viability in contrast to more intricate approaches like Incremental Conductance and metaheuristic techniques like PSO. Because humidity-induced losses are not negligible in tropical and subtropical climates, it is therefore ideal for small-scale or embedded PV systems but slow transient behaviour of this method is one of the limitations. Therefore, there exists a potential avenue for future research to develop more streamlined controllers that achieve greater speed and enhanced accuracy through the adoption of alternative algorithms. The outcomes of the present study are anticipated to significantly contribute to further research in hardware validation and real-time adaptation to varying loads and diverse climatic conditions. Future studies may also emphasize the significance of integrated thermal management strategies, such as phase-change materials and advanced cooling techniques to reduce thermal losses and enhance overall system efficiency.

REFERENCES

[1] L. Olatomiwa, H. O. Idakwo, W. S. Olusola, and C. Ezeh, “Global energy consumption trends,” *Majlesi Journal of Electrical Engineering*, vol. 19, no. 1, 2025, doi: 10.57647/j.mjee.2025.1901.09.

[2] A. Luque and S. Hegedus, *Handbook of Photovoltaic Science and Engineering*, 2nd ed. Chichester, U.K.: Wiley, 2011, doi: 10.1002/9780470974704.

[3] A. Y. Al-Hasan and A. A. Ghoneim, “A new correlation between photovoltaic panel’s efficiency and amount of sand dust accumulated on their surface,” *International Journal of Sustainable Energy*, vol. 24, no. 4, pp. 187–197, 2005, doi: 10.1080/14786450500291834.

[4] D. S. Hasan and M. S. Farhan, “Impact of cloud, rain, humidity, and wind velocity on PV panel performance,” *Wasit Journal of Engineering Science*, vol. 10, no. 2, pp. 34–43, 2022, doi: 10.31185/ejuow.vol10.iss2.237.

[5] M. A. Green, *Solar Cells: Operating Principles, Technology, and System Applications*. Englewood Cliffs, NJ, USA: Prentice-Hall, 1982.

[6] S. Dubey, J. N. Sarvaiya, and B. S. Seshadri, “Temperature dependent photovoltaic (PV) efficiency and its effect on PV production in the world–a review,” *Energy Procedia*, vol. 33, pp. 311–321, 2013, doi: 10.1016/j.egypro.2013.05.072.

[7] A. H. Rajpar, M. B. Bashir, E. Y. Salih, E. M. Ahmed, and A. M. Soliman, "Efficiency enhancement of photovoltaic–thermoelectric generator hybrid module by heat dissipating technique," *Results in Engineering*, vol. 23, no. 102907, 2024, doi: 10.1016/j.rineng.2024.102907.

[8] H. J. Goldsmid, *Introduction to Thermoelectricity*. Berlin, Germany: Springer, 2010, doi: 10.1007/978-3-642-00716-3.

[9] G. J. Snyder and E. S. Toberer, "Complex thermoelectric materials," *Nature Materials*, vol. 7, no. 2, pp. 105–114, 2008, doi: 10.1038/nmat2090.

[10] H. Mamur, O. F. Dilmaç, J. Begum, and M. R. Bhuiyan, "Thermoelectric generators act as renewable energy sources," *Cleaner Materials*, vol. 2, p. 100030, 2021, doi: 10.1016/j.clema.2021.100030.

[11] N. Kanagaraj, "Photovoltaic and thermoelectric generator combined hybrid energy system with an enhanced maximum power point tracking technique for higher energy conversion efficiency," *Sustainability*, vol. 13, no. 6, p. 3144, 2021, doi: 10.3390/su13063144.

[12] K. El Kamouny *et al.*, "Thermoelectric cooling micro-inverter for PV application," *Solar Energy Materials and Solar Cells*, vol. 180, pp. 311–321, 2018, doi: 10.1016/j.solmat.2017.06.061.

[13] K. Ilse, B. Figgis, M. Z. Khan, V. Naumann, and C. Hagendorf, "Dew as a detrimental influencing factor for soiling of PV modules," *IEEE Journal of Photovoltaics*, vol. 9, no. 1, pp. 287–294, 2019, doi: 10.1109/JPHOTOV.2018.2882649.

[14] R. T. Hamdi, S. A. Hafad, H. A. Kazem, and M. T. Chaichan, "Humidity impact on photovoltaic cells performance: A review," *International Journal of Recent Engineering Research and Development*, vol. 3, no. 11, pp. 27–37, 2018. [Online]. Available: https://www.ijrerd.com/papers/v3-i11/5-IJRERD-C264.pdf

[15] F. A. Touati, M. A. Al-Hitmi, and H. J. Bouchech, "Study of the effects of dust, relative humidity, and temperature on solar PV performance in Doha: Comparison between monocrystalline and amorphous PVs," *International Journal of Green Energy*, vol. 10, no. 7, pp. 680–689, 2013, doi: 10.1080/15435075.2012.727113.

[16] R. Lamba and S. C. Kaushik, "Modeling and performance analysis of a concentrated photovoltaic–thermoelectric hybrid power generation system," *Energy Conversion and Management*, vol. 115, pp. 288–298, 2016, doi: 10.1016/j.enconman.2016.02.061.

[17] A. Z. Sahin *et al.*, "A review on the performance of photovoltaic/thermoelectric hybrid generators," *International Journal of Energy Research*, vol. 44, no. 5, pp. 3365–3394, 2020, doi: 10.1002/er.5139.

[18] S. S. Indira *et al.*, "A review on various configurations of hybrid concentrator photovoltaic and thermoelectric generator system," *Solar Energy*, vol. 201, pp. 122–148, 2020, doi: 10.1016/j.solener.2020.02.090.

[19] M. A. Qasim *et al.*, "Conversion of heat generated during normal PV panel operation into useful energy via a hybrid PV–TEG connection," *International Journal of Renewable Energy Research*, vol. 12, no. 4, pp. 1779–1786, 2022, doi: 10.33019/jurnalecotipe.v11i2.4522.

[20] H. F. Kohan, F. Lotfipour, and M. Eslami, “Numerical simulation of a photovoltaic thermoelectric hybrid power generation system,” *Solar Energy*, vol. 174, pp. 537–548, 2018, doi: 10.1016/j.gloei.2023.10.005.

[21] Akbari and S. H. Keshmiri, “Efficiency enhancement of a tandem perovskite–silicon solar cell,” *Majlesi Journal of Electrical Engineering*, vol. 18, no. 3, pp. 1–7, 2024, doi: 10.57647/j.mjee.2024.180349.

[22] M. Padmanaban *et al.*, “Extensive study on online, offline and hybrid MPPT algorithms for photovoltaic systems,” *Majlesi Journal of Electrical Engineering*, vol. 15, no. 3, pp. 1–16, 2021, doi: 10.52547/mjee.15.3.1.

[23] A. Ghelam, M. Boudiaf, and Y. Derouiche, “Correction of the photovoltaic system control by the addition of a voltage regulator in the electrical conversion chain,” *Majlesi Journal of Electrical Engineering*, vol. 14, no. 3, pp. 45–52, 2020, doi: 10.29252/mjee.14.3.5.

[24] B. Yang, R. Xie, J. Duan, and J. Wang, “State-of-the-art review of MPPT techniques for hybrid PV–TEG systems: Modeling, methodologies, and perspectives,” *Global Energy Interconnection*, vol. 6, no. 5, pp. 567–591, 2023, doi: 10.1016/j.gloei.2023.10.002.

[25] M. Brahmi, C. Regaya, H. Hichem, and A. Zaafouri, “Comparative study of P&O and PSO particle swarm optimization MPPT controllers under partial shading,” *International Journal of Electrical and Computer Engineering*, vol. 4, pp. 45–50, 2022, doi: 10.37394/232027.2022.4.7.

[26] M. Bayat, M. Samkan, and H. Moeinpour, “A new maximum power point tracking method for photovoltaic system under partial shading conditions,” *Majlesi Journal of Electrical Engineering*, vol. 10, no. 2, pp. 17–29, 2016.

[27] M. K. Senapati, C. Pradhan, S. Padmanaban, and O. A. Zaabi, “Photovoltaic MPPT performance adaptability to partial shading resilience and load variations with modified adaptive Jaya optimization,” *IEEE Transactions on Consumer Electronics*, 2025, doi: 10.1109/TCE.2025.3532660.

[28] M. K. Senapati, C. Pradhan, and R. K. Calay, “A computational intelligence based maximum power point tracking for photovoltaic power generation system with small-signal analysis,” *Optimal Control Applications and Methods*, vol. 44, no. 2, 2023, doi: 10.1002/oca.2798.

[29] M. K. Senapati *et al.*, “Standalone PV system by using bio-inspired based MPPT technique,” in *Sustainable Energy and Technological Advancements*, ISSETA 2023, *Advances in Sustainability Science and Technology*. Singapore: Springer, 2023, pp. 431–444, doi: 10.1007/978-981-99-4175-9_35.

[30] C. Pradhan, M. K. Senapati, N. K. Ntiakoh, and R. K. Calay, “Roach infestation optimization MPPT algorithm for solar photovoltaic system,” *Electronics*, vol. 11, no. 6, p. 927, 2022, doi: 10.3390/electronics11060927.

[31] M. Ahmadi, M. H. Mousavi, M. Hassan, and R. Kumars, “A new approach for harmonic detection based on eliminating oscillatory coupling effects in microgrids,” *IET Renewable Power Generation*, vol. 17, 2023, doi: 10.1049/rpg2.12867.

[32] N. Kanagaraj, H. Rezk, and M. R. Gomaa, “A variable fractional order fuzzy logic control based MPPT technique for improving energy conversion efficiency of thermoelectric power generator,” *Energies*, vol. 13, no. 17, p. 4531, 2020, doi: 10.3390/en13174531.

[33] K. Safaei, A. Esmaeilian-Marnani, H. Emami, and A. H. Zaeri, “Fuzzy controller optimized by the grasshopper algorithm to realize maximum power in photovoltaic systems,” *Majlesi Journal of Electrical Engineering*, vol. 19, no. 1, pp. 1–8, 2025, doi: 10.57647/j.mjee.2025.1901.02.

[34] R. A. Muhammed and D. Sulaiman, “Particle swarm optimization (PSO) based MPPT controller modeling and design of photovoltaic modules,” *Majlesi Journal of Electrical Engineering*, vol. 16, no. 4, pp. 167–175, 2022, doi: 10.30486/mjee.2023.1970258.0.

[35] L. Jaklair, G. Yesuratnam, and P. M. Sarma, “Control algorithm for renewable energy standalone system with power quality and demand management,” *Majlesi Journal of Electrical Engineering*, vol. 18, no. 1, 2024, doi: 10.30486/mjee.2024.2006726.1363.

[36] W. Wu *et al.*, “Interfacial advances yielding high efficiencies for thermoelectric devices,” *Journal of Materials Chemistry*, vol. 9, no. 6, pp. 3209–3230, 2021, doi: 10.1039/D0TA06471H.

[37] R. Dhawan *et al.*, “Maximizing performance of microelectronic thermoelectric generators with parasitic thermal and electrical resistances,” *IEEE Transactions on Electron Devices*, vol. 68, no. 5, pp. 2434–2439, 2021, doi: 10.1109/TED.2021.3067624.

[38] M. A. V. Rad *et al.*, “Critical analysis of enhanced photovoltaic thermal systems: A comparative experimental study of PCM, TEG, and nanofluid applications,” *Energy Conversion and Management*, vol. 314, p. 118712, 2024, doi: 10.1016/j.enconman.2024.118712.

[39] J. Wang, Y. Li, B. Yang, and L. Jiang, “Multi-optimized reconfiguration of hybrid photovoltaic–thermoelectric generation (PV–TEG) system for performance enhancement,” *Energy Conversion and Management*, vol. 307, p. 118373, 2024, doi: 10.1016/j.enconman.2024.118373.

[40] S. Mitterhofer *et al.*, “Measurement and simulation of moisture ingress in PV modules in various climates,” *IEEE Journal of Photovoltaics*, 2023, doi: 10.1109/JPHOTOV.2023.3323808.

[41] A. K. Tripathi, S. Ray, M. Aruna, and S. Prasad, “Evaluation of solar PV panel performance under humid atmosphere,” *Materials Today: Proceedings*, vol. 45, pp. 5916–5920, 2021, doi: 10.1016/j.matpr.2020.09.682.

[42] M. G. Lawrence, “The relationship between relative humidity and the dewpoint temperature in moist air: A simple conversion and applications,” *Bulletin of the American Meteorological Society*, vol. 86, no. 2, pp. 225–234, 2005, doi: 10.1175/BAMS-86-2-225.

[43] V. J. Chin, Z. Salam, and K. Ishaque, “Cell modelling and model parameters estimation techniques for photovoltaic simulator application: A review,” *Applied Energy*, vol. 154, pp. 500–519, 2015, doi: 10.1016/j.apenergy.2015.05.035.

[44] H. Jouhara *et al.*, “Thermoelectric generator (TEG) technologies and applications,” *International Journal of Thermofluids*, vol. 9, p. 100063, 2021, doi: 10.1016/j.ijft.2021.100063.

[45] B. Ryu *et al.*, “Best thermoelectric efficiency of ever-explored materials,” *iScience*, vol. 26, no. 4, p. 106494, 2023, doi: 10.1016/j.isci.2023.106494.

[46] R. Bjork and K. K. Nielsen, “The performance of a combined solar photovoltaic (PV) and thermoelectric generator (TEG) system,” *Solar Energy*, vol. 120, pp. 187–194, 2015, doi: 10.1016/j.solener.2015.07.035.

[47] A. F. Mirza *et al.*, “High-efficiency hybrid PV–TEG system with intelligent control to harvest maximum energy under various non-static operating conditions,” *Journal of Cleaner Production*, vol. 320, p. 128643, 2021, doi: 10.1016/j.jclepro.2021.128643.

[48] S. Ibrahim *et al.*, “Linear regression model in estimating solar radiation in Perlis,” *Energy Procedia*, vol. 18, pp. 1402–1412, 2012, doi: 10.1016/j.egypro.2012.05.156.

[49] M. Ejaz, “Optimal control of hybrid photovoltaic–thermoelectric generator system using GEPSO,” *Journal of Power and Energy Engineering*, vol. 10, no. 3, pp. 1–21, 2022, doi: 10.4236/jpee.2022.103001.

[50] A. D. Dhass, N. Beemkumar, S. Harikrishnan, and H. M. Ali, “A review on factors influencing the mismatch losses in solar photovoltaic system,” *International Journal of Photoenergy*, vol. 2022, pp. 1–27, 2022, doi: 10.1155/2022/2986004.

[51] H. Abidi, L. Sidhom, and I. Chihi, “Systematic literature review and benchmarking for photovoltaic MPPT techniques,” *Energies*, vol. 16, no. 8, p. 3509, 2023, doi: 10.3390/en16083509.